DE GRUYTER Nanotechnology Reviews 2023; 12: 20220571

Review Article

Wei Zhang*

An overview of the synthesis of silicon carbide–boron carbide composite powders

https://doi.org/10.1515/ntrev-2022-0571
received June 23, 2022; accepted June 28, 2023

Abstract: Recently, silicon carbide–boron carbide composite ceramics have attracted more and more attention. The most important achievements of the silicon carbide–boron carbide composite ceramics should be applied in terms of mechanical, physical, and chemical for use in various advanced industries, such as armor plates, nozzles, abrasive tools, mechanical seals, *etc.* To prepare silicon carbide–boron carbide composite ceramics with good performance, the synthesis of silicon carbide–boron carbide composite powders is the basis. The synthesis approaches of silicon carbide–boron carbide composite powders are systematically summarized in this review, including ball milling, high-energy ball milling, self-propagating high-temperature synthesis (SHS), and sol–gel. Particularly, nanosized silicon carbide–boron carbide composite powders can be *in situ* synthesized by high-energy ball milling, SHS, or sol–gel. When commercial silicon carbide and/or boron carbide powders are used as raw materials to synthesize silicon carbide–boron carbide composite powders, the pretreatment of acid etching can significantly remove oxide layers existing on the surfaces of initial powders.

Keywords: silicon carbide, boron carbide composite powders, nanosize, ball milling, high-energy ball milling, self-propagating high-temperature synthesis, sol–gel

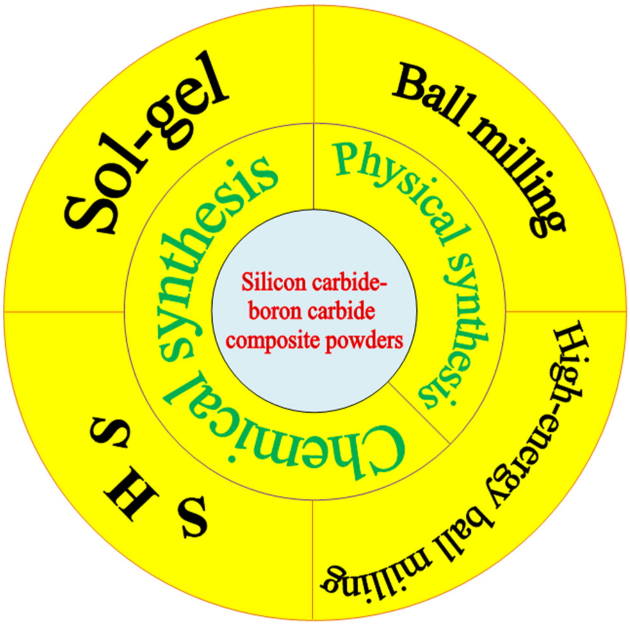

Graphical abstract

1 Introduction

Today, refractory carbides are of particular importance, and their application is rapidly growing. This is not only because of their commercial aspects but also due to their refractory applications and abrasion resistance, including cutting and abrasive tools. In addition to their appropriate chemical resistance, these carbides have high hardness and thermal resistance. They are important non-oxide ceramics, widely used in tools, abrasion-resistant materials, aerospace industries, microelectronics, as an amplifier in super-alloys and composites, wall protective layer of nuclear reactors, absorbent of environmental pollutants, *etc.* [1–3].

Silicon carbide and boron carbide are of some good physical performance, such as high melting point (2,700°C for silicon carbide, 2,427°C for boron carbide), low density (3.21 g/cm^3 for silicon carbide, 2.52 g/cm^3 for boron carbide), high hardness (24 GPa for silicon carbide, 36 GPa for boron carbide), and high elastic modulus (400 GPa for silicon carbide, 450 GPa for boron carbide) [4–9]; both of silicon carbide and boron carbide have good wear resistance [10–12]. In particular, silicon carbide has low thermal expansion coefficient, high thermal conductivity, and good oxidation resistance [13,14]; boron carbide possesses good neutron absorption capability [15,16]. Silicon carbide and boron carbide are widely applied in engineering fields due to their good performance.

Because of the good properties of silicon carbide and boron carbide, they are often used together to prepare

---

* **Corresponding author: Wei Zhang,** Department of Chemical Systems Engineering, Graduate School of Engineering, Nagoya University, Nagoya 4648603, Japan, e-mail: cnzhangwei2008@126.com

silicon carbide–boron carbide composite ceramics. The silicon carbide–boron carbide binary system can provide a combination of high hardness, low density, and relatively high fracture toughness. Silicon carbide–boron carbide composite ceramics have a wide application (Figure 1), such as armor plates, turbine engines, heat-conducting tubes, nozzles, abrasive tools, sliding bearings, thrust bearings, and mechanical seals [17–22].

Silicon carbide–boron carbide composite ceramics have outstanding properties and wide applications; thus, silicon carbide–boron carbide composite ceramics have received considerable scientific attention in recent years. To prepare silicon carbide–boron carbide composite ceramics, the synthesis of silicon carbide–boron carbide composite powders is the basis. The performance of silicon carbide–boron carbide composite powders, such as particle dispersion uniformity, purity, and particle size, will determine the properties of silicon carbide–boron carbide composite ceramics. Therefore, it is important to study the synthesis of silicon carbide–boron carbide composite powders. Different from the synthesis of single-component powders, the dispersion uniformity of two-component particles is particularly important for the synthesis of two-component powders. Previously, a lot of work has been done on the synthesis of individual silicon carbide powders and individual boron carbide powders [23–26]; however, the research on the synthesis of silicon carbide–boron carbide composite powders has received widespread attention recently. At present, the main synthesis approaches of silicon carbide–boron carbide composite powders include direct mixing of commercial silicon carbide and boron carbide powders by ball milling or high-energy ball milling as well as *in situ* synthesis by high-energy ball milling, self-propagating high-temperature synthesis (SHS), and sol–gel. Particularly, high-energy ball milling, SHS, and sol–gel are approaches to synthesizing silicon carbide–boron carbide composite powders with nanosize *in situ*. When commercial silicon carbide and boron carbide powders are used as raw materials, prior to synthesizing silicon carbide–boron carbide composite powders, silicon carbide and boron carbide raw materials can be pretreated to remove oxide layers existing on the surfaces of initial silicon carbide and boron carbide powders. The present work aims to summarize the available literature on the synthesis of silicon carbide–boron carbide composite powders, which can provide some theoretical basis and guidance for the synthesis of silicon carbide–boron carbide composite powders and the preparation of silicon carbide–boron carbide composite ceramics.

Figure 1: Applications of silicon carbide–boron carbide composite ceramics.

2 Pretreatment of raw materials

For non-oxide ceramic raw materials like silicon carbide and boron carbide, oxide layers usually exist on their surfaces [27,28]. The thickness of the oxide layer is affected by many factors, such as the humidity of the air and the particle size of the powder [29,30]. These oxide layers on the non-oxide ceramic raw materials would cause grain coarsening and are not beneficial to the densification of the obtained ceramics during the subsequent sintering [31]. When commercial silicon carbide and/or boron carbide powders are used as raw materials to synthesize silicon carbide–boron carbide composite powders, it is necessary to pre-treat the raw materials. Usually, adding carbon into silicon carbide–boron carbide composite powders can remove these oxide layers from silicon carbide and boron carbide powders by the reactions between carbon and SiO_2 and between carbon and B_2O_3, respectively, during the subsequent sintering at high temperatures [32,33]; however, if the amount of oxygen of silicon carbide and boron carbide starting powders is too high, more carbon would be added into silicon carbide–boron carbide composite powders, which can result in the reduction in the hardness of the obtained silicon carbide–boron carbide composite ceramics [34]. To remove the oxide layers from silicon carbide and boron carbide powders, the commercial silicon carbide and boron carbide raw materials can be pretreated before the synthesis of silicon carbide–boron carbide composite powders.

To reduce the oxygen amount of silicon carbide and boron carbide raw materials, acid etching is an effective method. Yaşar and Haber [35] used 50% hydrofluoric acid (HF) and diluted hydrochloric acid (HCl) to wash silicon carbide and boron carbide raw materials, respectively. After acid etching, the oxygen content of silicon carbide starting powders is reduced from 1.69 to 0.66 wt%, and the oxygen content of boron carbide starting powders is reduced from 2.90 to 1.70 wt%. Acid etching to silicon carbide and boron carbide raw materials can significantly reduce their oxygen contents, but it cannot completely remove their oxide layers. Furthermore, the particle sizes of silicon carbide powders before and after acid etching are 0.65 and 0.60 μm, respectively, and the particle sizes of boron carbide powders are 0.60 μm before and after etching. This indicates that the acid etching process would not significantly change the particle sizes of silicon carbide and boron carbide raw materials. In addition, to synthesize silicon carbide–boron carbide composite powders, Wang *et al.* [36] also used HF and HCl to wash silicon carbide whiskers and boron carbide powders to remove SiO_2 and B_2O_3, respectively; Hwang *et al.* [37] used $HCl–H_2O$ solution to wash boron carbide starting powders before synthesizing silicon carbide–boron carbide composite powders. For the subsequent mixing process, the acid-etched silicon carbide and/or boron carbide powders are used to synthesize silicon carbide–boron carbide composite powders.

The pretreatment of acid etching to silicon carbide and boron carbide raw materials can significantly remove their oxide layers, which is a method to obtain silicon carbide–boron carbide composite powders with low oxygen content and can also lay the foundation for the preparation of dense silicon carbide–boron carbide composite ceramics during the subsequent sintering.

3 Synthesis approaches of silicon carbide–boron carbide composite powders

To obtain silicon carbide–boron carbide composite ceramics with high relative density and good properties, the synthesis of silicon carbide–boron carbide composite powders is the foundation and prerequisite. The technology for producing composite powders usually involves mixing two or more finely dispersed powder systems. The popular synthesis approaches of silicon carbide–boron carbide composite powders include ball milling, high-energy ball milling, SHS, and sol–gel.

3.1 Ball milling

Ball milling is a common approach to preparing composite powders by directly mixing multi-component powders. Generally, composite powders can be prepared from multiple single-component powders by dry mixing or wet mixing. The common preparation approach of silicon carbide–boron carbide composite powders is the direct mixing of commercial silicon carbide and boron carbide powders by ball milling (Figure 2) [38–41]. Usually, silicon carbide and boron carbide powders obtained through industrial manufacturing are micron-sized. During the ball milling, the sizes of both silicon carbide and boron carbide powders are hardly changed due to low ball milling energy and the high hardness of silicon carbide and boron carbide particles. In general, the size of silicon carbide–boron carbide composite powders synthesized by ball milling is submicron/micron, which depends on the initial size of the raw materials. It is hard to fabricate dense silicon carbide–boron carbide composite ceramics from these composite powders with the size of submicron/micron; thus, various sintering additives are added to mix with silicon carbide and boron carbide powders together during the ball milling to promote the subsequent sintering.

The synthesis of silicon carbide–boron carbide composite powders by ball milling involves mixing two finely dispersed powder systems. If the silicon carbide–boron carbide composite powders synthesized by ball milling are uneven, the properties of the silicon carbide–boron carbide composite ceramics produced by the consolidation of such composite powders would be significantly degraded. Dry mixing and wet mixing are two methods to mix silicon carbide powders and boron carbide powders by ball milling. Wet ball milling is adding solvent when mixing silicon carbide powders and boron carbide powders, such as ethanol and water. In contrast, dry ball milling is the mixing of silicon carbide powders and boron carbide powders without additional solvent. Compared with the silicon carbide–boron carbide composite powders synthesized by dry mixing, the silicon carbide–boron carbide composite powders synthesized by wet mixing are more uniform and are more conducive to

Figure 2: Procedure of ball milling.

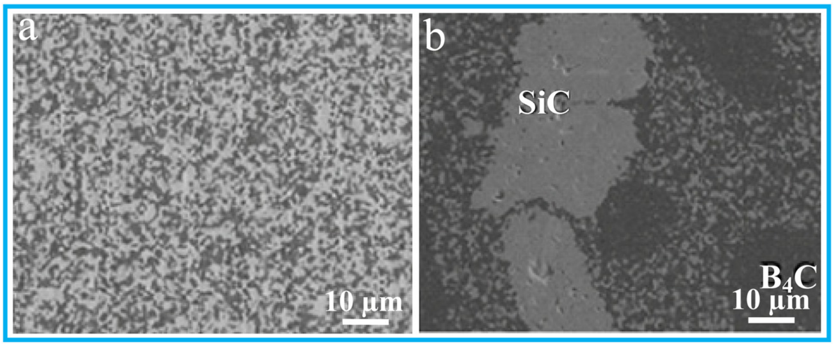

Figure 3: Microstructures of spark plasma sintered silicon carbide–50 wt% boron carbide composite ceramics produced from silicon carbide–boron carbide composite powders synthesized by: (a) wet ball milling and (b) dry mixing [35].

obtaining silicon carbide–boron carbide composite ceramics with good structural uniformity and high relative density [35]. Yaşar and Haber [35] noted that the relative densities of the spark plasma sintered silicon carbide–50 wt% boron carbide composite ceramics produced from the silicon carbide–boron carbide composite powders synthesized by wet ball milling and dry mixing are 98.9 and 97.5%, respectively; meanwhile, the silicon carbide–boron carbide composite powders synthesized by wet ball milling can provide a more uniform microstructure for the resulting silicon carbide–boron carbide composite ceramics (Figure 3(a)), whereas large pockets of individual components exist in the silicon carbide–boron carbide composite ceramics prepared from the silicon carbide–boron carbide composite powders synthesized by dry mixing (Figure 3(b)). The agglomerates of individual components in the silicon carbide–boron carbide composite ceramics resulting from the dry mixing of silicon carbide powders and boron carbide powders would cause an effect on the mechanical properties of the resulting silicon carbide–boron carbide composite ceramics. With the increase of boron carbide content in the resulting silicon carbide–boron carbide composite ceramics from 10 to 50 wt%, the hardness, fracture toughness, Young's modulus, shear modulus, bulk modulus, and Poisson's ratio of the silicon carbide–boron carbide composite ceramics produced from the silicon carbide–boron carbide composite powders synthesized by wet ball milling show a trend, *i.e.*, the hardness increases, and the fracture toughness, Young's modulus, shear modulus, bulk modulus, and Poisson's ratio decrease; however, the hardness, fracture toughness, Young's modulus, shear modulus, bulk modulus, and Poisson's ratio of the silicon carbide–boron carbide composite ceramics prepared from the silicon carbide–boron carbide composite powders synthesized by dry mixing do not exhibit a regular trend due to the inefficient mixing. Furthermore, Zhang *et al.* [42–44], So *et al.* [45], and Matović *et al.* [46] also noted that the silicon carbide–boron carbide composite powders synthesized by wet ball milling can provide a good particle dispersion for the obtained pressureless sintered silicon carbide–boron carbide composite ceramics (Figure 4(a)), hot-press sintered silicon carbide–boron carbide composite ceramics (Figure 4(b)), and ultra-high pressure sintered silicon carbide–boron carbide composite ceramics, respectively (Figure 4(c)).

In brief, the silicon carbide–boron carbide composite powders synthesized by ball milling of silicon carbide powders and boron carbide powders basically maintain the

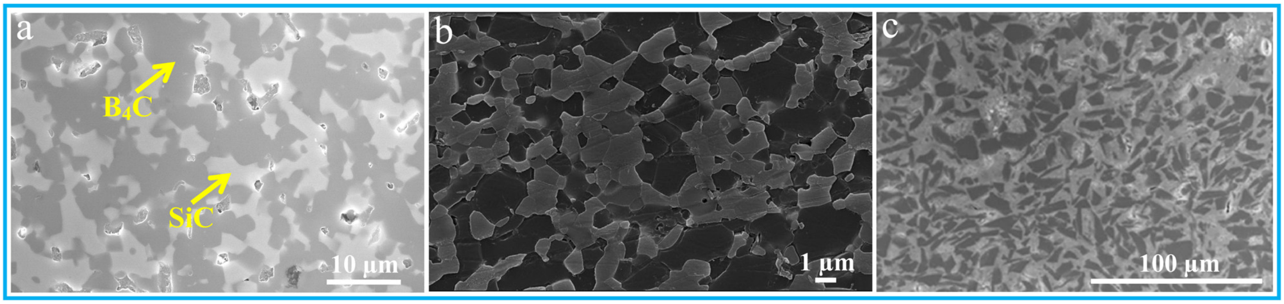

Figure 4: Microstructures of silicon carbide–boron carbide composite ceramics produced from silicon carbide–boron carbide composite powders synthesized by wet ball milling: (a) pressureless sintered 40 wt% silicon carbide–60 wt% boron carbide composite ceramics [43], (b) hot-press sintered 50 wt% silicon carbide–50 wt% boron carbide composite ceramics [45], (c) ultra-high pressure sintered 50 wt% silicon carbide–50 wt% boron carbide composite ceramics [46].

original characteristics of the raw materials, and the silicon carbide powders and boron carbide powders are just uniformly mixed. Until now, due to the advantages of simplicity, convenience, and low cost, direct ball milling of commercial silicon carbide and boron carbide powders is the most widely used approach to synthesizing silicon carbide–boron carbide composite powders [34,47–65]. Therefore, this approach is very suitable for the industrial synthesis of silicon carbide–boron carbide composite powders. However, ball milling is not suitable for synthesizing silicon carbide–boron carbide nanocomposite powders because the agglomeration of silicon carbide nanoparticles and boron carbide nanoparticles is difficult to be broken by ball milling, resulting in the inhomogeneous distribution of silicon carbide nanopowders and boron carbide nanopowders in the synthesized silicon carbide–boron carbide nanocomposite powders. This significantly degrades the performance of final silicon carbide–boron carbide nanocomposite ceramics prepared by the consolidation of such composite powders.

3.2 High-energy ball milling

The basic principle of high-energy ball milling, which is also called mechanical alloying, is to use mechanical energy to induce chemical reactions or to induce changes in the structure and properties of materials. Different from common ball milling, high-energy ball milling can reduce the particle size of the milled materials in the repeated extruding and crushing process due to high ball milling energy. More importantly, high-energy ball milling is an approach to synthesizing ultrafine powders with a disordered structure, resulting in the formation of a number of lattice defects and the change of stoichiometric ratio [66]. Although lattice defects are increased in the synthesized powders, such powders with a disordered structure have higher sintering activity.

3.2.1 Synthesis of silicon carbide–boron carbide composite powders by direct high-energy ball milling of silicon carbide and boron carbide powders

Reducing the particle sizes of silicon carbide and boron carbide raw materials is one of the effective methods to promote the sintering of silicon carbide–boron carbide composite ceramics. Another strategy is to make the silicon carbide–boron carbide composite powders produce a disordered structure, which can be realized during the high-energy ball milling, so as to enhance the sintering activity of the silicon carbide–boron carbide composite powders. Silicon carbide–boron carbide composite powders with reduced particle size and disordered structure can be synthesized by high-energy ball milling of silicon carbide and boron carbide powders.

Zhang *et al.* [67] used silicon carbide and boron carbide raw materials with a mass ratio of 1:1 whose initial particle sizes are 2.57 and 3.11 μm, respectively, to synthesize silicon carbide–boron carbide composite powders by high-energy ball milling in Ar gas. The number of small particles increases, and the particles gradually tend to be homogenized in the synthesized silicon carbide–boron carbide composite powders by appropriately increasing the ball-powder mass ratio or prolonging the milling time [68]. After milling with the ball-powder mass ratio of 30:1 for 120 h, the mean particle size of silicon carbide–boron carbide composite powders reduces from 2.5 to 0.7 μm, and the morphology of the composite powders changes from irregular and sharp-edged shape to spheric shape with narrow size distribution (Figure 5(a) and (b)). As the milling time is more than 120 h, the particle size and the shape of silicon carbide–boron carbide composite powders are not changed with an increase in milling time (Figure 5(c)). After high-energy ball milling, some silicon carbide–boron carbide composite powders adhere together and agglomerate inevitably because of the increased activity of the powders and the heat released during the milling.

Moreover, although the silicon carbide and boron carbide raw materials have perfect crystallinity, the synthesized silicon carbide–boron carbide composite powders possess a disordered structure, indicating that the order-disorder transformation of silicon carbide–boron carbide composite powders occurs during the high-energy ball milling [67]. By comparison, the silicon carbide–boron carbide composite powders (0.7 μm) synthesized by wet ball milling have a perfect crystallinity; however, for the silicon carbide–boron carbide composite powders synthesized by high-energy ball milling, lattice defects are generated and the amorphous structure of silicon carbide and boron carbide is significantly increased. The crystal silicon carbide and boron carbide raw materials are not completely transformed into the amorphous structure owing to their high hardness and high bond energy of Si–C and B–C. The disordered structure of silicon carbide–boron carbide composite powders has an important effect on the subsequent sintering of silicon carbide–boron carbide composite ceramics. On the one hand, during the sintering, the disordered structure of silicon carbide–boron carbide composite powders can increase the molecular diffusion channel, which is favorable for the densification of the silicon carbide–boron

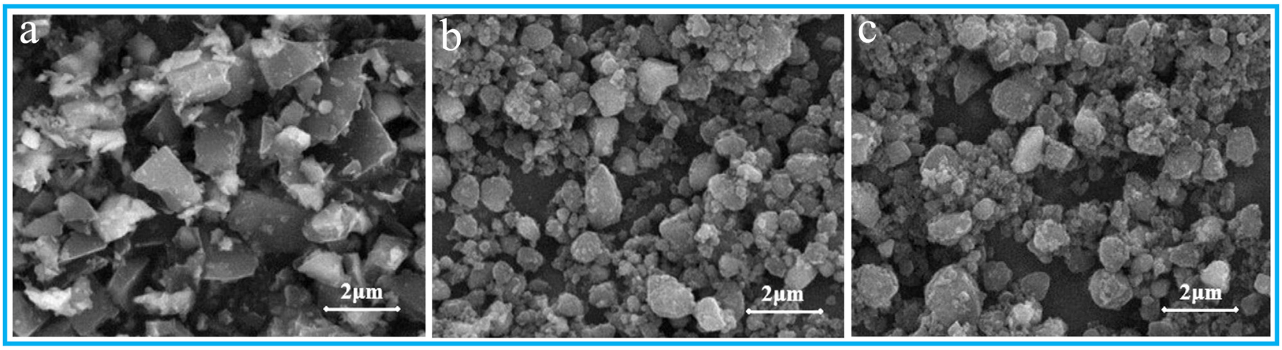

Figure 5: Silicon carbide–boron carbide composite powders: (a) starting mixture composed of silicon carbide and boron carbide particles, (b) after high-energy ball milling for 120 h, and (c) after high-energy ball milling for 160 h [67].

carbide composite ceramics. On the other hand, the disordered structure of the silicon carbide–boron carbide composite powders can be transformed into the ordered structure of the resulting silicon carbide–boron carbide composite ceramics during the sintering; the energy is released during the disorder-order transformation, which can serve as a driving force for the sintering. Therefore, the silicon carbide–boron carbide composite powders with the disordered structure synthesized by high-energy ball milling have high sintering activity, which is a feature different from the silicon carbide–boron carbide composite powders synthesized by ball milling.

Compared with the relative density of the hot-press sintered silicon carbide–boron carbide composite ceramics produced from the silicon carbide–boron carbide composite powders synthesized by wet ball milling, the relative density (96.4%) of the hot-press sintered silicon carbide–boron carbide composite ceramics produced from the silicon carbide–boron carbide composite powders synthesized by high-energy ball milling is 13% higher, and the microstructure of the silicon carbide–boron carbide composite ceramics produced from the silicon carbide–boron carbide composite powders synthesized by high-energy ball milling is denser (Figure 6) [67]. This demonstrates that the silicon carbide–boron carbide composite powders synthesized by high-energy ball milling have an improved sintering activity owing to their disordered structure. With the same particle size of silicon carbide–boron carbide composite powders and the same sintering process, the microstructure and relative density of the obtained silicon carbide–boron carbide composite ceramics produced from the silicon carbide–boron carbide composite powders synthesized by high-energy ball milling and ball milling are extremely disparate. The synthesized silicon carbide–boron carbide composite powders *via* high-energy ball milling can realize the preparation of dense hot-press sintered silicon carbide–boron carbide composite ceramics under relatively low temperatures without any sintering additive. As a result, the resulting silicon carbide–boron carbide composite ceramics produced from the silicon carbide–boron carbide composite powders synthesized by high-energy ball milling can obtain improved mechanical properties; the flexural strength, hardness, and fracture toughness can reach 430 MPa, 24.5 GPa, and 4.6 MPa $m^{1/2}$, respectively.

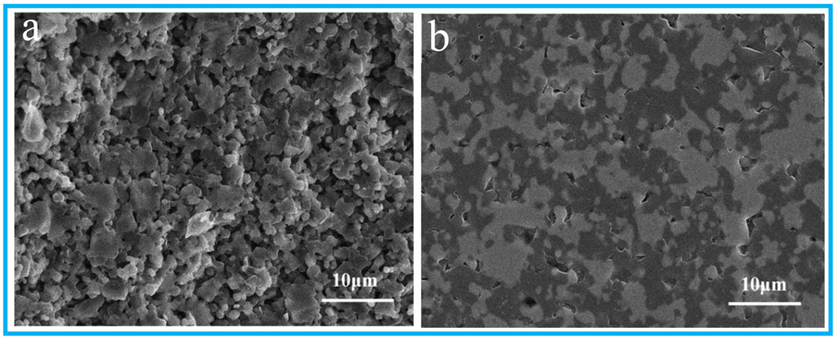

Figure 6: Hot-press sintered silicon carbide–boron carbide composite ceramics at 1,950°C produced from the silicon carbide–boron carbide composite powders synthesized by: (a) ball milling and (b) high-energy ball milling [67].

3.2.2 *In situ* synthesis of silicon carbide–boron carbide composite powders by high-energy ball milling

Although silicon carbide–boron carbide composite powders can be synthesized using commercial silicon carbide and boron carbide as raw materials *via* high-energy ball milling, the average particle size of silicon carbide–boron carbide composite powders is submicron, which is attributed to the high hardness of silicon carbide and boron carbide particles. In order to fabricate nanosized silicon carbide–boron carbide composite powders, Zhang *et al.* [69] used boron carbide (3 μm), softer Si (200 mesh), and amorphous carbon (1 μm) as raw materials and increased the ball milling energy to *in situ* synthesize silicon carbide–boron carbide nanocomposite powders by high-energy ball milling in Ar gas. The mixture of starting raw materials is of micron size with a large size distribution range, and the shape of particles is sharp-edged and irregular (Figure 7(a)). After high-energy ball milling, the composite powders are composed of nanocrystalline boron carbide (5–20 nm) with an increased volume of lattice defects and amorphous silicon carbide. The crystal boron carbide raw material is not completely transformed into an amorphous structure owing to its high hardness and high bond energy of B–C. There are no amorphous Si and amorphous C in the synthesized silicon carbide–boron carbide composite powders. The particle size of the synthesized silicon carbide–boron carbide composite powders is 50–150 nm with a homogeneous distribution, and the silicon carbide–boron carbide composite powders are sphere-like (Figure 7(b)). The synthesized silicon carbide–boron carbide composite powders are of a nanoscaled size and disordered structure; as a result, they have high sintering activity. The silicon carbide component in the synthesized nanosized silicon carbide–boron carbide composite powders is formed from C and Si *via* mechanochemical processing (Si + C → SiC); thus, using boron carbide, amorphous carbon, and Si powders as raw materials *via* high-energy ball milling is a novel approach to *in situ* synthesizing homogeneously dispersed silicon carbide–boron carbide nanocomposite powders composed of amorphous silicon carbide and nanocrystalline boron carbide. Correspondingly, the resulting silicon carbide–boron carbide composite ceramics produced from these nanosized silicon carbide–boron carbide composite powders *in situ* synthesized by high-energy ball milling exhibit higher relative density (98.6%), hardness (34.3 GPa), and fracture toughness (6.0 MPa m$^{1/2}$) compared to the silicon carbide–boron carbide composite ceramics produced from the silicon carbide–boron carbide composite powders synthesized by direct high-energy ball milling of silicon carbide and boron carbide powders.

For the synthesis of nanocomposite powders *via* high-energy ball milling, there are two reaction mechanisms during synthesis. One is the gradual diffusion reaction, and the other is the mechanically induced self-propagation reaction [70]. The mechanically induced self-propagation reaction mechanism exists in the highly exothermic system and is related to high-temperature reactions. Because of the ball-to-ball and ball-to-powder collisions during high-energy ball milling, the local temperature may be higher than the ignition temperature; thus, the combustion reaction would occur regionally, resulting in the complete synthesis of the crystalline products in a short time at the local high temperature. Also, a large number of ignition events occur during the milling. As a result, the mechanically induced self-propagating reaction is a massive and explosive process during high-energy ball milling. For the gradual diffusion-reaction mechanism, the powders around the colliding balls first undergo severe plastic deformation; then, the flattened particles contact with clean surfaces, forming the composite powders through gradual diffusion of thin layers. This formation process is gradual and slow. Accordingly, the product synthesized through the gradual diffusion reaction has an amorphous structure rather than a crystal structure.

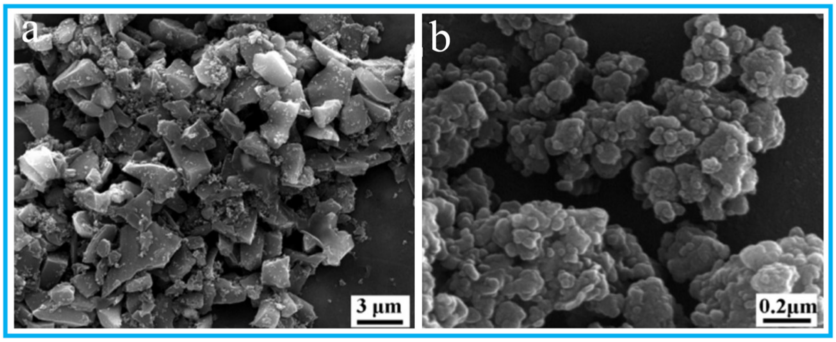

Figure 7: *In situ* synthesized silicon carbide–boron carbide nanocomposite powders: (a) starting mixture composed of boron carbide, Si, and amorphous carbon and (b) after high-energy ball milling for 96 h [69].

For the synthesis of single-phase silicon carbide particles *via* high-energy ball milling using Si and C, both the gradual diffusion reaction mechanism and the mechanically induced self-propagation reaction mechanism work because both crystal and amorphous silicon carbide structures exist in the products [71,72]. However, for the synthesis of silicon carbide–boron carbide composite powders, the solid-state reactions between Si and C are highly diluted due to the existence of boron carbide powders when boron carbide, Si, and C powders are milled together by high-energy ball milling, hindering the formation of crystal silicon carbide. The dilution of reactants increases the ignition temperature required for the explosion reaction and significantly decreases the reaction rate. As a result, the mechanically induced self-propagation reaction of silicon carbide is hindered by the dilution of reactants, although silicon carbide is prone to undergo self-propagating synthesis. Therefore, the reaction mechanism of silicon carbide–boron carbide composite powders synthesized by high-energy ball milling with boron carbide, Si, and amorphous carbon as raw materials is only controlled by the gradual diffusion reaction mechanism [73]. In the high-energy ball milling process, the powders of C and Si are rapidly refined to generate nanocrystalline and amorphous phases with high defect density, allowing the large clear interface area, high driving force, high diffusion rate, and short diffusion path for the diffusion of C atoms into the interstices of Si lattice to form an interstitial solid solution Si (C). A severe lattice distortion is implied in Si (C) lattice because of the large mismatch of the structure and atomic radius between C and Si. This lattice distortion of Si (C) is improved with an increase in milling time, resulting in the destruction of the distorted chemical bond of Si–Si; thus, C atoms located in interstices of Si lattice gradually occupy the positions of Si to generate amorphous silicon carbide with an increase in milling time [73]. Generally, the solid solubility rate of C atoms into the interstices of Si is about 0 due to a little larger radius of Si atoms (0.1172 nm) than that of C atoms (0.0914 nm); however, it can be greatly extended due to the function of mechanical force and the large volume of grain boundaries in the high-energy ball milling process. No Si and C atoms dissolve into the interstices of the boron carbide lattice or occupy the positions of B or C atoms in boron carbide to generate a solid solution due to the high bond energy of B–C and the saturation of C atoms in boron carbide (the B/C ratio of 4:1) [73].

In brief, high-energy ball milling is a simple, industrial, practical, economically variable but powerful approach to synthesizing nano/submicron-sized silicon carbide–boron carbide composite powders with a disordered structure. In particular, the silicon carbide–boron carbide nanocomposite powders can be synthesized *in situ* through solid-solid reactions *via* high-energy ball milling. The changes in raw materials during the high-energy ball milling include the generation of lattice defects to increase disordered structure and the reduction in particle size; thus, the synthesized silicon carbide–boron carbide composite powders possess higher sintering activity, which can increase sintering energy and reduce sintering temperature for the preparation of silicon carbide–boron carbide composite ceramics. During the subsequent sintering, the silicon carbide–boron carbide composite powders with disordered structures are transformed into the final silicon carbide–boron carbide composite ceramics with ordered structure. The released power during the disorder-order transformation serves as a sintering driving force and is beneficial to sintering. Meanwhile, the structural disorder-order transformation can enhance mass transport [74]. In this way, dense silicon carbide–boron carbide composite ceramics can be produced under lower sintering temperatures. These characteristics of the silicon carbide–boron carbide composite powders synthesized by high-energy ball milling cannot be achieved by other technologies. Therefore, the silicon carbide–boron carbide composite powders synthesized by high-energy ball milling have also been widely used in the production of silicon carbide–boron carbide composite ceramics [33,75–81]. In addition, it is worth noting that if the high-energy ball milling is carried out in the air, extra B_2O_3 that is detrimental to densification would be generated on the surface of boron carbide nanocrystals [82]. To eliminate the oxide film on the silicon carbide–boron carbide composite powders formed during the high-energy ball milling in air, annealing post-treatment in Ar is an effective approach [82,83]. However, the annealing post-treatment is only to eliminate the oxygen impurities formed during the high-energy ball milling in air, and it cannot provide oxygen-free powders due to the spontaneous passivation of boron carbide in contact with air.

3.3 SHS

SHS is an approach for the rapid synthesis of materials, during which thermal energy of exothermic reactions can result in the synthesis of materials and the self-combustion wave propagation through the whole of a sample [84]. During SHS, high-speed heating and cooling of materials can cause various defects in the synthesized materials. For materials with kinetic and/or thermodynamic limitations for reactions, they require activation prior to SHS. The commonly used activation methods mainly include electric field activation, mechanical activation, chemical oven, and preheat. Mechanical activation (high-energy ball milling) is a simple and effective way of activation. On the one hand, mechanical activation can not only reduce the particle size of raw materials but also produce defects on the surface of raw materials, leading to increased system energy, decreased ignition temperature, and faster combustion velocity [85,86]; on the other hand, due to the high reaction rate of SHS, the changes made for raw materials by mechanical activation are influential even after the synthesis [87,88]. Meanwhile, various defects caused by high-speed heating and cooling in the synthesized powders during SHS are favorable for reducing the sintering temperature of the subsequent ceramic preparation.

3.3.1 Preparation process, synthesis mechanism, and characteristics of silicon carbide–boron carbide composite powders synthesized by SHS

The exothermic reaction formation of silicon carbide and boron carbide from their elements is so low that the synthesis of silicon carbide–boron carbide composite powders *via* SHS is difficult [89]. Thus, mechanical activation is needed to improve synthesis conditions before the SHS of silicon carbide–boron carbide composite powders. In addition to mechanical activation, the reduction reaction of B_2O_3 by Mg, which is an exothermic reaction, can also be used to synthesize silicon carbide–boron carbide composite powders *in situ*. That is, element B is not used as the raw material directly; instead, element B is generated through the reduction reaction of B_2O_3 by Mg, and the thermal energy released by this exothermic reaction is the primary source of heating for the synthesis of silicon carbide–boron carbide composite powders *via* SHS route. Based on this, Roghani *et al.* [90] used B_2O_3, Mg, Si, and graphite powders as starting materials to *in situ* synthesize silicon carbide–boron carbide composite powders with a molar ratio of 1:1 *via* the SHS approach, which is according to the following reaction:

$$2B_2O_3 + Si + 2C + 6Mg \rightarrow B_4C + SiC + 6MgO. \quad (1)$$

Reaction (1) is composed of the following three separate reactions:

$$B_2O_3 + 3Mg \rightarrow 2B + 3MgO, \quad (2)$$

$$4B + C \rightarrow B_4C, \quad (3)$$

$$Si + C \rightarrow SiC. \quad (4)$$

Before the synthesis of silicon carbide–boron carbide composite powders, the powder mixture is first subjected to high-energy ball milling as an activation process, during which the grain sizes of reactants are reduced, the microstrain is induced, and the defect density in the mixed powders is increased; thus, the system energy increases, and the subsequent reactions would be promoted kinetically. No new phases are generated during the mechanical activation. Appropriately adjusting the milling parameters, *i.e.*, increasing ball to powder ratio, prolonging milling time, and increasing rotation speed, can increase milling energy and microstrain, reduce grain size, decrease starting time of ignition, and increase combustion temperature; thus, a more complete synthesis of silicon carbide–boron carbide composite powders and the reduction in amounts of unreacted raw materials can be achieved during the subsequent SHS [91]. Further, increasing the ball-to-powder ratio is more effective than prolonging the milling time to realize the aforementioned purpose. After combustion reactions, compared with the powder mixture composed of B_2O_3, Mg, Si, and graphite subjected to mechanical activation, the same powder mixture without mechanical activation contains raw materials of Si and graphite, but does not contain silicon carbide, indicating that the system energy is not enough for the generation of silicon carbide [92].

After the mechanical activation, the powder mixture is compacted and then subjected to combustion reactions in a tubular furnace at high temperatures (800–1,000°C) in an Ar atmosphere. Appropriately increasing the synthesis temperature can increase the system energy; thus, the particle size of the obtained composite powders is more uniform, and the agglomeration of particles is reduced. Furthermore, some unreacted melt Si phase surrounds the synthesized grains when the temperature is 800°C, but it would disappear as the temperature is increased to 900°C, indicating that the Si reacts completely and there is no residual Si in the system [90].

The synthesized composite powders after combustion reactions are porous and agglomerated particles, and the agglomerated particles with less than 10 μm consist of flake-like shaped and rough fine particles (Figure 8(a)). The synthesized composite powders after combustion reactions contain boron carbide, silicon carbide, magnesium oxide, magnesium borates, boron oxide, and residual carbon. According to reaction (1), MgO is synthesized in the composite powders; further, $Mg_2B_2O_5$ and $Mg_3B_2O_6$ byproducts also exist in the composite powders, which are generated by the reaction between generated MgO and remain unreduced B_2O_3 resulting from the insufficient Mg due to its evaporation during combustion reactions [93,94]. As a result, the reaction of boron carbide formation is incomplete. Thus, appropriately increasing the molar ratio of Mg to B_2O_3 can decrease the formation amount of $Mg_2B_2O_5$ and $Mg_3B_2O_6$ byproducts, which is attributed to the more complete reduction reaction of B_2O_3 by Mg [90]. Due to the evaporation of Mg in the

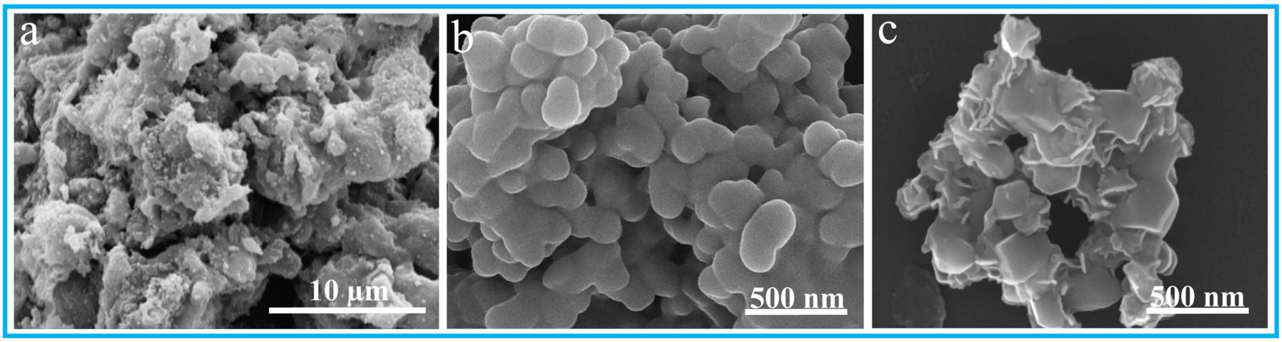

Figure 8: Silicon carbide–boron carbide composite powders synthesized *via* SHS in the tubular furnace: (a) after combustion reactions [92] and (b) after acid leaching [96]. (c) Silicon carbide–boron carbide composite powders synthesized *via* SHS in the spark plasma furnace after acid leaching [96].

combustion process, the use of more than the stoichiometric molar ratio of Mg to B_2O_3 (Mg/B_2O_3 molar ratio of 7:2) is suggested [90]. Furthermore, appropriately increasing the molar ratio of Mg to B_2O_3 can also reduce the amount of residual graphite and thus increase the amount of synthesized boron carbide in the final composite powders, resulting from the more complete reduction reaction of B_2O_3 by Mg and continuing reaction of generated B with graphite; more complete reduction reaction of B_2O_3 by Mg can result in more heat generation and higher combustion temperature.

To eliminate MgO, $Mg_2B_2O_5$, and $Mg_3B_2O_6$ in the composite powders after SHS, using HCl aqueous solution is an effective method to purify the silicon carbide–boron carbide composite powders synthesized by the SHS route. The elimination of MgO is according to the following reaction [95]:

$$MgO(s) + 2HCl(aq) \rightarrow MgCl_2(aq) + H_2O(l). \tag{5}$$

During the elimination, the magnesium borates are decomposed to MgO and B_2O_3 in the acidic solution; MgO can be dissolved in the acidic solution, while B_2O_3 remains in the amorphous form [92]. Therefore, amorphous B_2O_3 (approximately 1.9 wt%) exists in the final silicon carbide–boron carbide composite powders synthesized by SHS *via* the above-mentioned route. Further, some impurities with less than 2 wt% exist in the synthesized silicon carbide–boron carbide composite powders, such as Fe and Mg. The absence of Si proves the complete synthesis of silicon carbide; the existence of B_2O_3 illustrates that the maintenance of more heat within the system seems to be necessary for the complete synthesis of boron carbide. Therefore, the main compositions of the synthesized silicon carbide–boron carbide composite powders are silicon carbide, boron carbide, B_2O_3, and C. The synthesized silicon carbide–boron carbide composite powders cannot be purified by burning up to remove residual carbon because silicon carbide–boron carbide composite powders can react with O_2 in the air at 655°C [96].

The synthesized silicon carbide–boron carbide composite powders by SHS after acid leaching have high homogeneity; the silicon carbide–boron carbide composite powders are composed of polyhedral agglomerated particles; the agglomerated particle size of the synthesized silicon carbide–boron carbide composite powders is between 90 and 200 nm, and most of the grain size is less than 30 nm (Figure 8(b)) [92,96]. Thereby, the grains of the silicon carbide–boron carbide composite powders synthesized by SHS possess a uniformity of size and shape. The reasons that the particle size of the synthesized silicon carbide–boron carbide composite powders is less than those of raw materials and the grain size of the silicon carbide–boron carbide composite powders is nanoscale are attributed to the high homogeneity and decreased grain size caused by the high-energy ball milling, high rate of combustion reactions, low synthesis temperature, and the formation of silicon carbide and boron carbide in a network of the generated MgO, which can increase nucleation and prevent the excessive growth of silicon carbide and boron carbide grains. Meanwhile, the high homogeneity can prevent the abnormal growth of silicon carbide grains by boron carbide grains generated *in situ* and *vice versa*. Furthermore, the grain size of silicon carbide is larger than that of boron carbide in the synthesized silicon carbide–boron carbide composite powders. On the one hand, after the mechanical activation, Si is crystalline, while C and B_2O_3 are amorphous; thus, the raw materials for the synthesis of silicon carbide are coarser; on the other hand, the synthesis of silicon carbide is a one-step reaction according to reaction (4), whereas the synthesis of boron carbide occurs in two steps according to reactions (2) and (3); thus, silicon carbide has a higher chance to receive heat and more time for grain growth.

3.3.2 The effect of heat sources

Different heat sources will have different effects on the synthesis of silicon carbide–boron carbide composite powders. Besides the tubular furnace, the spark plasma furnace can also be used to synthesize silicon carbide–boron carbide composite powders. The combustion synthesis *via* a spark plasma furnace is not realized upon reaching the whole reactants at a specified temperature. Instead, it is accessed by forming enough heat at a certain point on the sample surface. Through the collision of spark plasma with the raw materials, the combustion reaction propagates within a fraction of a second in the raw material volume. The temperature in the spark plasma furnace is not expected to start synthesis effectively. Therefore, synthesis can be achieved at an ambient temperature by applying a specific current to raw materials in a spark plasma furnace. The spark plasma furnace can be used as a rapid heating method for the *in situ* synthesis of powder compounds under certain conditions.

Compared with the synthesized silicon carbide–boron carbide composite powders carried out in the tubular furnace, the silicon carbide–boron carbide composite powders synthesized *via* the spark plasma furnace can obtain a higher purity [96]. The amounts of residual B_2O_3 and C in the silicon carbide–boron carbide composite powders synthesized through the spark plasma furnace are significantly lower than those in the silicon carbide–boron carbide composite powders synthesized by the tubular furnace; thus, the synthesis of boron carbide in the silicon carbide–boron carbide composite powders is promoted by the spark plasma furnace. The purity of the silicon carbide–boron carbide composite powders synthesized through the spark plasma furnace increases with an increase in reactant volume. There are still less than 2 wt% impurities in the silicon carbide–boron carbide composite powders synthesized through the spark plasma furnace, such as O, Fe, and Mg. The higher purity of the silicon carbide–boron carbide composite powders synthesized by the spark plasma furnace is attributed to the decreased heat dissipation in the spark plasma furnace. First, the use of graphite die prevents particles from getting scattered and immunizes the reactants from heat dissipation. Second, using a higher reactant volume in the graphite die can cause a higher heat amount; thus, for the synthesis in the graphite die, the energy generated is greater than the heat dissipation. As a result, more heat promotes the synthesis of silicon carbide–boron carbide composite powders. Third, the high heating rate and applying appropriate current at a minimum time can prevent the differentiation of phases. In addition, it is worth noting that the materials with a high electrical conductivity that can dissipate created heat are not suitable for synthesis by the spark plasma furnace [97]. The successful synthesis of silicon carbide–boron carbide composite powders in the spark plasma furnace is attributed to their semiconductor nature.

Due to the decrease of amorphous residual B_2O_3, the agglomeration in the silicon carbide–boron carbide composite powders synthesized by the spark plasma furnace is reduced; meanwhile, using raw materials with a larger volume in the graphite die can generate a higher heat amount, resulting in the perfect synthesis of the silicon carbide–boron carbide composite powders. Therefore, the silicon carbide–boron carbide composite powders synthesized in the spark plasma furnace are composed of plate-like particles with a thickness of less than 100 nm and a diameter of 200–600 nm (Figure 8(c)). The grain size of the synthesized silicon carbide–boron carbide composite powders through the spark plasma furnace increases with an increase in reactant volume. Although the grain size of silicon carbide–boron carbide composite powders synthesized through the spark plasma furnace is larger than that of silicon carbide–boron carbide composite powders synthesized through the tubular furnace, which is attributed to the decreased thermal dissipation in the spark plasma furnace, the grain sizes of the silicon carbide–boron carbide composite powders synthesized by both heat sources are at the nanoscale.

In brief, silicon carbide–boron carbide composite powders can be synthesized *in situ via* the SHS approach. The synthesized silicon carbide–boron carbide composite powders have high homogeneity, and the grains with nanoscale possess a uniformity of size and shape. Further, various defects are caused in the synthesized silicon carbide–boron carbide composite powders because of the high-speed heating and cooling process, which can promote the subsequent sintering of silicon carbide–boron carbide composite ceramics. Although silicon carbide–boron carbide nanocomposite powders can be synthesized using B_2O_3, Mg, Si, and graphite powders as starting materials *via* SHS, MgO is dominant in the combustion reaction products (approximately 72 wt%). Therefore, the yield of silicon carbide–boron carbide nanocomposite powders synthesized by this route is relatively low. Also, silicon carbide–boron carbide composite powders synthesized by SHS need to be mechanically activated before the synthesis and also need acid leaching after the synthesis; thus, the synthesis process is relatively complex.

3.4 Sol–gel

Sol–gel is a chemical approach to synthesizing high-purity powders by using inorganic or organic precursor metallic materials (alkoxides). The most important characteristic of the final powder materials synthesized by the sol–gel route is the compositional homogeneity on a molecular scale. This is believed to be crucial merit for the synthesis of multi-component powders. Meanwhile, the fine and micron-sized powders can be prepared even without agglomeration by chemical precise procedures. In particular, the sol–gel route is one of the popular chemical approaches for the preparation of nanosized powders.

Although there are a few studies carried out on the synthesis of nano/submicron-sized single-phase silicon carbide and single-phase boron carbide powders by the sol–gel approach [98–102], the research on the synthesis of silicon carbide–boron carbide composite powders by sol–gel is quite limited. In fact, different from the synthesis of single-component powders *via* the sol–gel route, the synthesis of a binary system is more complex. Different hydrolysis rates of different components in the binary system can cause the segregation of materials in the final binary sol, leading to the formation of an inhomogeneous gel. This is a great challenge for the synthesis of binary system composite powders by the sol–gel route. The use of binary alkoxide materials as precursors of the sol–gel route is one of the effective ways to solve this problem. The binary alkoxides are hydrolyzed and polymerized in the same way as simple alkoxides, but the final gel would contain the same portion of two homogeneous metallic alkoxides at an atomic level. To avoid the above-mentioned influence caused by the different hydrolysis rates from the different components, a simple solution is proposed that the alkoxide precursor with a lower hydrolysis rate is first hydrolyzed in the sol; after a certain time, the other alkoxide with a higher hydrolysis rate is added to the sol. Consequently, not only are both alkoxides hydrolyzed at the same time but also the latter alkoxide is cross-linked with the first alkoxide [103].

Najafi *et al.* [104] utilized tetraethyl orthosilicate (TEOS), tetramethyl/borate (TMB), and phenolic resin as precursors for Si, B, and C, respectively, to synthesize silicon carbide–boron carbide nanocomposite powders *via* the sol–gel approach for the first time. Due to the faster hydrolysis rate of boron methoxide than that of TEOS, TEOS is first exposed to water before boron methoxide. According to reaction (6), the alkoxide undergoes partial hydrolysis and generates sialon groups. Then, these sialon groups are cross-linked together and create siloxane cross-linked groups according to reaction (7), indicating the gelation reaction. Subsequently, boron methoxide is added to the system. According to reaction (8), the hydrolysis of alkoxide precursor of B can occur, and the produced groups can also participate in condensation reactions and produce the polymeric network of reaction products according to reaction (9). However, atypical condensation reactions (reactions (10) and (11)) are faster as compared to self-condensation or typical condensation reactions (reactions (8) and (9)). As a result, these complex mixtures of different molecules (molecular groups of Si and B mixture) are more likely to be close to each other rather than in two separate systems, resulting from the dissimilar columbic charges existing in these binary systems. Therefore, materials absorb each other and get stabilized. Meanwhile, by adding a dispersant and controlling the pH in the sol, a homogenous gel with uniform chemical composition is finally obtained according to reactions (10) and (11). The heterogeneous growth of precursor particles or their agglomeration in the sol can be prevented by controlling the hydrolyzing and stabilizing agents; thus, the precursor particles of B and Si with a size of about 2.1 nm are synthesized, and this particle size is appropriate with homogeneous and narrow distribution. Most of all, the mixing of obtained precursor particles is on a molecular scale.

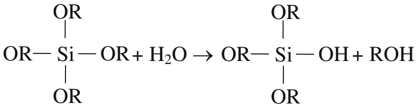

$$\mathrm{OR{-}\underset{OR}{\overset{OR}{Si}}{-}OR + H_2O \rightarrow OR{-}\underset{OR}{\overset{OR}{Si}}{-}OH + ROH} \tag{6}$$

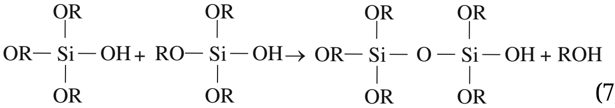

$$\mathrm{OR{-}\underset{OR}{\overset{OR}{Si}}{-}OH + RO{-}\underset{OR}{\overset{OR}{Si}}{-}OH \rightarrow OR{-}\underset{OR}{\overset{OR}{Si}}{-}O{-}\underset{OR}{\overset{OR}{Si}}{-}OH + ROH} \tag{7}$$

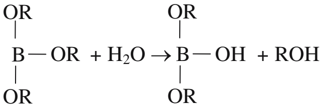

$$\mathrm{\underset{OR}{\overset{OR}{B}}{-}OR + H_2O \rightarrow \underset{OR}{\overset{OR}{B}}{-}OH + ROH} \tag{8}$$

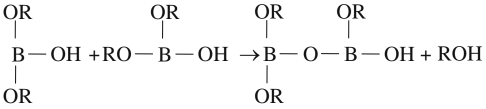

$$\mathrm{\underset{OR}{\overset{OR}{B}}{-}OH + RO{-}\overset{OR}{B}{-}OH \rightarrow \underset{OR}{\overset{OR}{B}}{-}O{-}\overset{OR}{B}{-}OH + ROH} \tag{9}$$

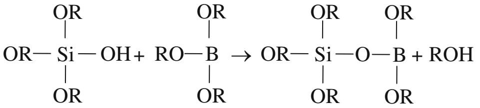

$$\mathrm{OR{-}\underset{OR}{\overset{OR}{Si}}{-}OH + RO{-}\underset{OR}{\overset{OR}{B}} \rightarrow OR{-}\underset{OR}{\overset{OR}{Si}}{-}O{-}\underset{OR}{\overset{OR}{B}} + ROH} \tag{10}$$

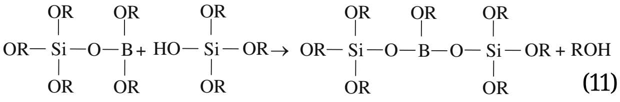

$$\mathrm{OR{-}\underset{OR}{\overset{OR}{Si}}{-}O{-}\underset{OR}{\overset{OR}{B}} + HO{-}\underset{OR}{\overset{OR}{Si}}{-}OR \rightarrow OR{-}\underset{OR}{\overset{OR}{Si}}{-}O{-}\overset{OR}{B}{-}O{-}\underset{OR}{\overset{OR}{Si}}{-}OR + ROH} \tag{11}$$

To obtain silicon carbide–boron carbide composite powders, it is necessary to heat the prepared gel powders. After heat treatment at 700°C in Ar atmosphere, no crystalline phase is formed; the XRD result confirms that the synthesized powders have an amorphous structure containing elemental Si, B, C, and O. However, after heat treatment at 1,350°C for 1 h, according to the XRD result, the primary nuclei of silicon carbide and boron carbide particles are formed; after heat treatment at 1,350°C for 2 h, the finally synthesized silicon carbide–boron carbide composite powders with spherical morphology are composed of β-silicon carbide and boron carbide, suggesting that silicon carbide and boron carbide particles can be formed simultaneously in the synthesized composite powders *via* the simultaneous hydrolysis synthesis method. The synthesis temperature is a decisive factor in the crystallization of silicon carbide–boron carbide composite powders from the precursor particles. The increased temperature and prolonged soaking time can make the precursor particles with an amorphous structure transform into silicon carbide–boron carbide composite powders with an ordered structure, which has been proved by the XRD analysis. The synthesized silicon carbide–boron carbide composite powders are uniform and have equiaxed grains; the particle size of the silicon carbide–boron carbide composite powders is 20–40 nm (Figure 9), and the particle distribution range is narrow. Also, the synthesized silicon carbide–boron carbide nanocomposite powders possess a high specific surface area of 171.42 m^2/g, and the surface of these nanocomposite powders is mesoporous. It is worth noting that there are still oxide surface layers composed of B_2O_3 and SiO_2 on the silicon carbide–boron carbide composite powders synthesized *via* this route.

In addition, Tkachenko *et al.* [105] developed a new technology to synthesize silicon carbide–boron carbide composite powders, in which silicon carbide–boron carbide composite powders can be obtained during the preparation of the mixture synthesized by a combined sol–gel and dissolution approach. A gel of silicic acid with as much saccharose as needed for the subsequent silicon carbide formation and an aqueous solution of boric acid with carbohydrates (saccharose) for a “solution” boron carbide are pre-prepared, respectively. The initial solution and gel are mixed in the specified ratio; as a result, the components are distributed with each other on a molecular level. Then water is removed from the solution by evaporation, and carbohydrates are pyrolyzed to supply a carbon source. The process temperature needs to be less than 600°C to prevent boron anhydride from melting, and the best temperature is the carbon caramelization point to maximize the carbon yield in coke residue. Carbide is produced in the subsequent stage. The synthesized silicon carbide–boron carbide composite powders are composed of three fractions according to the morphology and grain size – that is, equiaxial grains with 1–20 μm, platy and rod-shaped grains up to 10 μm thick and up to 100 μm long, and grains sintered into friable agglomerates with 50 μm in size, the grain size in which is 1–10 μm. The first two fractions belong to boron carbide, and the third fraction contains both β-silicon carbide and boron carbide phases. Furthermore, a graphite-like phase exists as an impurity in the synthesized silicon carbide–boron carbide composite powders. Although the agglomerates and the platy and rod-shaped particles exist in the initial resulting silicon carbide–boron carbide composite powders, these agglomerates and particles can be almost completely pulverized after grinding. Using these silicon carbide–boron carbide composite powders synthesized by this combined sol–gel and dissolution approach to produce the hot-press sintered 20 wt% silicon carbide–80 wt% boron carbide composite ceramics, the average grain sizes of silicon carbide and boron carbide in the ceramics are 2 and 5 μm, respectively. The fracture surface of the obtained silicon carbide–boron carbide composite ceramics shows the characteristic of transgranular fracture, and the fracture toughness is 6.1 MPa $m^{1/2}$.

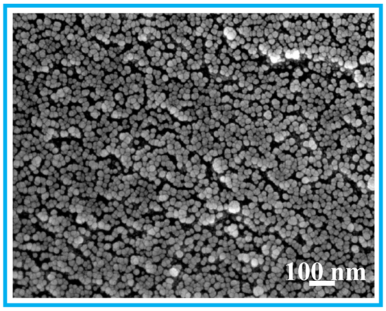

Figure 9: Silicon carbide–boron carbide composite powders synthesized by the sol–gel approach after heat treatment at 1,350°C for 2 h [104].

In brief, for the sol– gel approach to synthesizing silicon carbide–boron carbide composite powders, precursor materials for the subsequent formation of silicon carbide and boron carbide, or B, Si, and C are used. These precursor materials are dissolved and mixed in liquid solvent on a molecular scale, resulting in a very homogeneous and uniform mixing of the synthesized silicon carbide–boron carbide composite powders. Especially, the sol–gel approach can produce nanosized silicon carbide–boron carbide composite powders. In the silicon carbide–boron carbide composite powders synthesized by the sol–gel route, the ratio of silicon carbide to boron carbide can be adjusted by the number of precursors. The synthesized silicon carbide–boron carbide composite powders by the sol–gel approach are quite uniform and nanosized; however, this route is affected by certain key factors that should be controlled precisely and properly in the process, such as temperature, pH, and the number of dispersants. Meanwhile, it is necessary to prevent the separation of precursor materials for silicon carbide and boron carbide in the multi-component gel. All these factors must be controlled simultaneously to achieve a desired target silicon

Table 1: Characteristics of silicon carbide–boron carbide composite powders synthesized by different approaches

Raw materials	Synthesis approach	Mean particle size of synthesized composite powders	Main phase compositions of composite powders	Note	Ref.
Silicon carbide (0.65 μm), boron carbide (0.60 μm), carbon	Dry mixing	0.6 μm	Silicon carbide, boron carbide, carbon	The silicon carbide and boron carbide raw materials are acid etched before dry mixing	[35]
Silicon carbide (0.65 μm), boron carbide (0.60 μm), carbon	Wet ball milling (SiC ball, ethanol medium)	0.6 μm	Silicon carbide, boron carbide, carbon	The silicon carbide and boron carbide raw materials are acid etched before wet ball milling	[35]
Silicon carbide (0.8 μm), boron carbide (0.7 μm)	Wet ball milling (Al_2O_3 ball, alcohol medium)	0.7 μm	Silicon carbide, boron carbide	—	[67]
Silicon carbide (3.11 μm), boron carbide (2.57 μm)	High-energy ball milling (rotation speed of 250 rpm, stainless steel ball, ethanol medium, Ar gas)	0.7 μm	Amorphous silicon carbide, amorphous boron carbide	The possible Fe contamination is removed through leaching in HCl acid	[67]
Boron carbide (3 μm), Si (200 mesh), amorphous carbon (1 μm)	High-energy ball milling (rotation speed of 350 rpm, stainless steel ball, ethanol medium, Ar gas)	50–150 nm	Amorphous silicon carbide, nanocrystalline boron carbide with increased volume of lattice defects	The possible Fe contamination is removed through leaching in HCl acid	[69]
Graphite (50 μm), Si (150 μm), Mg (<100 μm), B_2O_3 (<50 μm)	SHS (tubular furnace, Ar gas, 1,000°C)	90–200 nm	β-Silicon carbide, boron carbide, B_2O_3, graphite	High-energy ball milling (rotation speed of 300 rpm, ball-to-powder ratio of 20:1, milling time of 12 h, stainless steel container, steel ball, and Ar gas) is used to activate the mixed raw materials. HCl acid leaching is used to remove byproducts	[92]
Graphite (<50 μm), Si (<250 μm), Mg (60–300 μm), B_2O_3	SHS (spark plasma furnace, graphite die with an inner diameter of 30 mm, Ar gas, 310°C)	237 nm	β-Silicon carbide, boron carbide, B_2O_3	The synthesis is carried out by applying a current under a pressure of about 10 MPa. HCl acid leaching is used to remove byproducts	[96]
TEOS, TMB, resol	Sol–gel (1,350°C × 2 h)	20–40 nm	β-Silicon carbide, boron carbide, B_2O_3, SiO_2	Ammonium polycarboxylate, DMF, and HCl are used as the dispersant, solvent, and catalyst, respectively	[104]
A gel of silicic acid with saccharose, an aqueous solution of boric acid with carbohydrates (saccharose)	Combination of dissolution and sol–gel (less than 600°C)	A wide range of grain size (from tens to hundreds of nanometers up to several micrometers)	β-Silicon carbide, boron carbide, a graphite-like phase	A gel of silicic acid with as much saccharose as necessary for the subsequent generation of silicon carbide is needed	[105]

Table 2: Advantages and disadvantages of each approach to synthesizing silicon carbide–boron carbide composite powders

Synthesis approach	Advantages	Disadvantages
Ball milling (dry)	Simplicity, convenience, low cost, and suitable for industrialization	Nonuniform mixing; not suitable for the synthesis of nanocomposite powders
Ball milling (wet)	Simplicity, convenience, low cost, uniform mixing, and suitable for industrialization	Long time-consuming; not suitable for the synthesis of nanocomposite powders
High-energy ball milling	Simplicity, convenience, low cost, and suitable for industrialization; uniform mixing; reduction in particle size; suitable for the synthesis of nanocomposite powders	Generation of contamination from tank and balls
SHS	Uniform mixing; suitable for the synthesis of nanocomposite powders	Complex process, low yield, and high cost
Sol–gel	Uniform mixing; suitable for the synthesis of nanocomposite powders	Complex process and high cost; hazardous precursors
Combination of dissolution and sol–gel	Uniform mixing	Complex process and high cost; uneven particle size; difficult to accurately control the amount of components

carbide–boron carbide composite powders with high homogeneity. Therefore, the sol–gel route is relatively complicated and cumbersome. Moreover, the advantage of the combination of dissolution and sol–gel approach to synthesizing silicon carbide–boron carbide composite powders is that the resulting silicon carbide particles and boron carbide particles can be dispersed very uniformly; but the disadvantage of this approach is that the rapid heating during the pyrolysis process can remove large amounts of carbon in the form of volatile radicals so that the content of resulting carbon reductant is undeterminable and the results of subsequent carbidization are ambiguous. Thereby, it is difficult to accurately control the amount of silicon carbide and boron carbide formed in the synthesized composite powders. Finally, it is also worth expecting and considering to develop non-hazardous and inexpensive precursor materials for silicon carbide–boron carbide composite powders [106].

4 Summary

For the silicon carbide–boron carbide composite ceramics, good particle dispersion of silicon carbide and boron carbide is very important, especially considering mechanical properties. Achieving this goal depends on the synthesis of silicon carbide–boron carbide composite powders. Silicon carbide–boron carbide composite powders can be synthesized in several approaches. The characteristics of silicon carbide–boron carbide composite powders synthesized by different approaches are summarized in Table 1. The advantages and disadvantages of each approach to synthesizing silicon carbide–boron carbide composite powders are summarized in Table 2. Silicon carbide–boron carbide composite powders can be synthesized by either physical methods, *i.e.*, directly mixing silicon carbide and boron carbide powders, or *in situ* chemical synthesis methods. The physical methods to synthesize silicon carbide–boron carbide composite powders include ball milling and high-energy ball milling; the chemical synthesis methods to synthesize silicon carbide–boron carbide composite powders include high-energy ball milling, SHS, and sol–gel. One of the most important properties of composite powders is uniformity. Compared with the silicon carbide–boron carbide composite powders synthesized by physical methods, the silicon carbide–boron carbide composite powders synthesized by chemical methods can obtain a more uniform particle dispersion. Especially, the silicon carbide and boron carbide particles are distributed in each other on a molecular scale in the silicon carbide–boron carbide composite powders synthesized *via* SHS and sol–gel routes.

In addition, nanosized silicon carbide–boron carbide composite powders are usually *in situ* synthesized by high-energy ball milling, SHS, or sol–gel. The highly active silicon carbide–boron carbide nanocomposite powders lay the foundation for the preparation of silicon carbide–boron carbide nanocomposite ceramics. On the one hand, using the nanosized silicon carbide–boron carbide composite powders can reduce the sintering temperature of silicon carbide–boron carbide nanocomposite ceramics because nanosized silicon carbide–boron carbide composite powders have shorter diffusion length among atoms and higher surface energy; on the other hand, silicon carbide–boron carbide nanocomposite ceramics can obtain better structural homogeneity and higher fracture toughness by using the nanosized silicon carbide–boron carbide composite powders. Generally, the silicon carbide-–boron carbide nanocomposite ceramics with better structural uniformity and mechanical properties are produced from the *in situ* synthesized silicon carbide–boron carbide nanocomposite powders, rather than from the milling of nanosized silicon carbide powders and nanosized boron carbide powders. Silicon carbide–boron carbide nanocomposite ceramics are the result of the combination of silicon carbide–boron carbide nanocomposite powders and ceramic sintering technology. The successful synthesis of silicon carbide–boron carbide nanocomposite powders expands the application field of advanced silicon carbide–boron carbide composite ceramics to a new direction and height.

Funding information: The author states no funding involved.

Author contributions: The author has accepted responsibility for the entire content of this manuscript and approved its submission.

Conflict of interest: The author states no conflict of interest.

References

[1] Najafi A, Fard FG, Rezaie HR. Sol-gel synthesis and characterization of B_4C nanopowder. Ceram Int. 2018;44(17):21386–94.

[2] Najafi A, Khoeini M, Jamshidi A. Manufacturing of nano mullite-silicon carbide filters by *in situ* reaction bonding. Ceram Int. 2020;46(10):15935–42.

[3] Sharifi F, Mahmoodi Z, Abbasi SM, Najafi A, Khalaj G. Synthesis and characterization of mesoporous TiC nanopowder/nanowhisker with low residual carbon processed by sol-gel method. J Mater Res Technol. 2023;22:2462–72.

[4] Thévenot F. Boron carbide- a comprehensive review. J Eur Ceram Soc. 1990;6(4):205–25.

[5] Suri AK, Subramanian C, Sonber JK. Murthy TSRCh. Synthesis and consolidation of boron carbide: A review. Int Mater Rev. 2010;55(1):4–40.

[6] Zhang W, Yamashita S, Kita H. Progress in pressureless sintering of boron carbide ceramics-A review. Adv Appl Ceram. 2019;118(4):222–39.

[7] Chen SL, Li WJ, Li XX, Yang WY. One-dimensional SiC nanostructures: Designed growth, properties, and applications. Prog Mater Sci. 2019;104:138–214.

[8] Zhang W, Yamashita S, Kumazawa T, Ozeki F, Hyuga H, Kita H. Tribological properties of B_4C ceramics prepared by pressureless sintering and annealed at different temperatures. Tribol Trans. 2020;63(4):672–82.

[9] Wang C, Zhou JW, Song M, Lu ZS, Chen XH, Zheng Y, et al. Synthesis of ultrafine silicon carbide nanoparticles using nonthermal arc plasma at atmospheric pressure. J Am Ceram Soc. 2021;104(8):3883–94.

[10] Zhang W, Yamashita S, Kita H. Progress in tribological research of SiC ceramics in unlubricated sliding-A review. Mater Des. 2020;190:108528.

[11] Zhang W. A review of tribological properties for boron carbide ceramics. Prog Mater Sci. 2021;116:100718.

[12] Zhang W. Tribology of SiC ceramics under lubrication: Features, developments and perspectives. Curr Opin Solid State Mater Sci. 2022;26(4):101000.

[13] Zhang W, Dai WY, Chiyoda N. Research on thermal shock resistance of mullite-bauxite-silicon carbide castable refractory. Chin J Geochem. 2012;31(2):204–8.

[14] Zhang W, Yamashita S, Kita H. Self lubrication of pressureless sintered SiC ceramics. J Mater Res Technol. 2020;9(6):12880–8.

[15] Sharifi EM, Karimzadeh F, Enayati MH. Mechanochemical assisted synthesis of B_4C nanoparticles. Adv Powder Technol. 2011;22(3):354–8.

[16] Zare A, He MR, Straker M, Chandrashekhare MVS, Spencer M, Hemker KJ, et al. Mechanical characterization of boron carbide single crystals. J Am Ceram Soc. 2022;105(5):3030–42.

[17] Gonzalez LV, Speyer RF. Flexural strength, fracture toughness, and hardness of silicon carbide and boron carbide armor ceramics. Int J Appl Ceram Technol. 2010;7(5):643–51.

[18] Paris V, Frage N, Dariel MP, Zaretsky E. The spall strength of silicon carbide and boron carbide ceramics processed by spark plasma sintering. Int J Impact Eng. 2010;37(11):1092–9.

[19] Zhang W, Yamashita S, Kita H. Tribological properties of SiC-B_4C ceramics under dry sliding condition. J Eur Ceram Soc. 2020;40(8):2855–61.

[20] Zhang W, Chen XY, Yamashita S, Kubota M, Kita H. B_4C–SiC ceramics with interfacial nanorelief morphologies and low underwater friction and wear. ACS Appl Nano Mater. 2021;4(3):3159–66.

[21] Zhang CP, Xia Q, Han LF, Zhao YL, Huang N, Ren QX, et al. Fabrication of carbon-coated boron carbide particle and its role in the reaction bonding of boron carbide by silicon infiltration. J Eur Ceram Soc. 2022;42(3):860–8.

[22] Zhang W. A novel ceramic with low friction and wear toward tribological applications: Boron carbide-silicon carbide. Adv Colloid Interface Sci. 2022;301:102604.

[23] Sinha A, Mahata T, Sharma BP. Carbothermal route for preparation of boron carbide powder from boric acid–citric acid gel precursor. J Nucl Mater. 2002;301(2–3):165–9.

[24] Ding DH, Bai B, Xiao GQ, Luo JY, Chong XC. Molten-salt-assisted combustion synthesis of B_4C powders: Synthesis mechanism and dielectric and electromagnetic wave absorbing properties. Ceram Int. 2021;47(13):18708–19.

[25] Wu CC, Gao T, Nie JF, Jiang L, Liu XF. In-situ synthesis of nano SiC particles in Al–Si–C system at 750°C. J Mater Res Technol. 2021;13:716–26.

[26] Zeraati M, Kazemzadeh P, Barani M, Sargazi G. Selecting the appropriate carbon source in the synthesis of SiC nanopowders using an optimized fuzzy model. Silicon. 2022;14(6):2953–64.

[27] Xu CM, Cai YB, Flodström K, Li ZS, Esmaeilzadeh S, Zhang GJ. Spark plasma sintering of B_4C ceramics: The effects of milling medium and TiB_2 addition. Int J Refract Met Hard Mater. 2012;30(1):139–44.

[28] Yasar ZA, Haber R. Effect of acid etching time and concentration on oxygen content of powder on the microstructure and elastic properties of silicon carbide densified by SPS. Int J Mater Sci Appl. 2020;9(1):7–13.

[29] Roy J, Chandra S, Das S, Maitra S. Oxidation behaviour of silicon carbide- A review. Rev Adv Mater Sci. 2014;38:29–39.

[30] Jia QL, Zhang HJ, Li SP, Jia XL. Effect of particle size on oxidation of silicon carbide powders. Ceram Int. 2007;33(2):309–13.

[31] Yaşar ZA, DeLucca VA, Haber RA. Influence of oxygen content on the microstructure and mechanical properties of SPS SiC. Ceram Int. 2018;44(18):23248–53.

[32] Kakiage M, Tominaga Y, Yanase I, Kobayashi H. Synthesis of boron carbide powder in relation to composition and structural homogeneity of precursor using condensed boric acid-polyol product. Powder Technol. 2012;221:257–63.

[33] Moshtaghioun BM, Ortiz AL, García DG, Rodríguez AD. Toughening of super-hard ultra-fine grained B_4C densified by spark-plasma sintering via SiC addition. J Eur Ceram Soc. 2013;33(8):1395–401.

[34] Lin WS, Fang NX. Mechanical properties and microstructure of reaction sintering B_4C/SiC ceramics. Appl Mech Mater. 2011;66–68:510–5.

[35] Yaşar ZA, Haber RA. Evaluating the role of uniformity on the properties of B_4C–SiC composites. Ceram Int. 2021;47(4):4838–44.

[36] Wang JL, Lin WS, Jiang ZW, Duan LH, Yang GL. The preparation and properties of SiC_w/B_4C composites infiltrated with molten silicon. Ceram Int. 2014;40(5):6793–8.

[37] Hwang C, Yang QR, Xiang SS, Domnich V, Khan AU, Xie KY, et al. Fabrication of dense B_4C-preceramic polymer derived SiC composite. J Eur Ceram Soc. 2019;39(4):718–25.

[38] Zhang W, Yamashita S, Kumazawa T, Ozeki F, Hyuga H, Kita H. Study on friction behavior of SiC-B_4C composite ceramics after annealing. Ind Lubr Tribol. 2020;72(5):673–9.

[39] Zhang W, Yamashita S, Kumazawa T, Ozeki F, Hyuga H, Kita H. Influence of surface roughness parameters and surface morphology on friction performance of ceramics. J Ceram Soc Jpn. 2019;127(11):837–42.

[40] Chen W, Hao WH, Zhao ZQ, He NR, Li XQ, Li HQ. Mechanical properties and tribological characteristics of B_4C-SiC ceramic composite in artificial seawater. J Asian Ceram Soc. 2021;9(4):1495–505.

[41] Jamale S, Kumar BVM. Sintering and sliding wear studies of B_4C-SiC composites. Int J Refract Met Hard Mater. 2020;87:105124.

[42] Zhang W, Yamashita S, Kita H. Effect of counterbody on tribological properties of B_4C-SiC composite ceramics. Wear. 2020;458–459:203418.

[43] Zhang W, Chen XY, Yamashita S, Kubota M, Kita H. Tribological behavior of B_4C-SiC composite ceramics under water lubrication: Influence of counterpart. Mater Sci Technol. 2021;37(9):863–76.

[44] Zhang W, Yamashita S, Kita H. Effects of load on tribological properties of B_4C and B_4C-SiC ceramics sliding against SiC balls. J Asian Ceram Soc. 2020;8(3):586–96.

[45] So SM, Choi WH, Kim KH, Park JS, Kim MS, Park J, et al. Mechanical properties of B_4C–SiC composites fabricated by hot-press sintering. Ceram Int. 2020;46(7):9575–81.

[46] Matović B, Maletaškić J, Prikhna T, Urbanovich V, Girman V, Lisnichuk M, et al. Characterization of B_4C-SiC ceramic composites prepared by ultra-high pressure sintering. J Eur Ceram Soc. 2021;41(9):4755–60.

[47] Magnani G, Beltrami G, Minoccari GL, Pilotti L. Pressureless sintering and properties of αSiC-B_4C composite. J Eur Ceram Soc. 2001;21(5):633–8.

[48] Aroati S, Cafri M, Dilman H, Dariel MP, Frage N. Preparation of reaction bonded silicon carbide (RBSC) using boron carbide as an alternative source of carbon. J Eur Ceram Soc. 2011;31(5):841–5.

[49] Sahin FC, Apak B, Akin I, Kanbur HE, Genckan DH, Turan A, et al. Spark plasma sintering of B_4C–SiC composites. Solid State Sci. 2012;14(11–12):1660–3.

[50] Zhang YL, Zhang YM, Hu M, Song XG. Effect of B_4C content on densification behavior of SiC-B_4C ceramics. Adv Mater Res. 2014;997:454–6.

[51] Sun HB, Zhang YJ, Li QS. Preparation and characterization of reaction sintering B_4C/SiC composite ceramic. Key Eng Mater. 2014;602–603:536–9.

[52] Vandeperre LJ, Teo JH. Pressureless sintering of SiC-B_4C composites. Advances in Ceramic Armor IX; 2014. p. 101–8.

[53] Zhang YL, Zhang YM, Li CH, Li JP. Influence of reaction temperature on the densification behavior of the SiC/B_4C composites. Appl Mech Mater. 2015;727–728:11–4.

[54] Guo WM, Xiao HN, Liu JX, Liang JJ, Gao PZ, Zeng GM. Effects of B_4C on the microstructure and phase transformation of porous SiC ceramics. Ceram Int. 2015;41(9):11117–24.

[55] Du XW, Wang Y, Zhang ZX, Zhang F, Wang WM, Fu ZY. Effects of silicon addition on the microstructure and properties of B_4C–SiC composite prepared with polycarbosilane-coated B_4C powder. Mater Sci Eng A. 2015;636:133–7.

[56] Zhou YC, Ni DW, Kan YM, He P, Dong SM, Zhang XY. Microstructure and mechanical properties of reaction bonded B_4C-SiC composites: The effect of polycarbosilane addition. Ceram Int. 2017;43(8):5887–95.

[57] Zhang XR, Zhang ZX, Wang WM, Che HW, Zhang XL, Bai YM, et al. Densification behaviour and mechanical properties of B_4C–SiC intergranular/intragranular nanocomposites fabricated through spark plasma sintering assisted by mechanochemistry. Ceram Int. 2017;43(2):1904–10.

[58] Moradkhani A, Baharvandi H. Mechanical properties and fracture behavior of B_4C-nano/micro SiC composites produced by pressureless sintering. Int J Refract Met Hard Mater. 2018;70:107–15.

[59] Zhang W, Yamashita S, Kumazawa T, Ozeki F, Hyuga H, Kita H. Effect of nanorelief structure formed *in situ* on tribological properties of ceramics in dry sliding. Ceram Int. 2019;45(11):13818–24.

[60] Zhang W, Yamashita S, Kumazawa T, Ozeki F, Hyuga H, Norimatsu W, et al. A study on formation mechanisms of relief structure formed *in situ* on the surface of ceramics. Ceram Int. 2019;45(17):23143–8.

[61] Li CR, Li S, An D, Xie ZP. Microstructure and mechanical properties of spark plasma sintered SiC ceramics aided by B_4C. Ceram Int. 2020;46(8):10142–6.

[62] Zhang W, Yamashita S, Kita H. A study of B_4C-SiC composite for self-lubrication. J Am Ceram Soc. 2021;104(5):2325–36.

[63] Zhang W, Chen XY, Yamashita S, Kubota M, Kita H. Effect of water temperature on tribological performance of B_4C-SiC ceramics under water lubrication. Tribol Lett. 2021;69(2):34.

[64] Zhang L, Ren XP, Li JK, Dong CC. Microstructure and mechanical properties of spark plasma sintered SiC–B_4C gradient ceramics with Al additive. Ceram Int. 2021;47(21):30844–51.

[65] Zhang W, Chen XY, Yamashita S, Kubota M, Kita H. Frictional characteristics of carbide ceramics in water. J Tribol. 2022;144(1):011702.

[66] Zhang DL. Processing of advanced materials using high-energy mechanical milling. Prog Mater Sci. 2004;49(3–4):537–60.

[67] Zhang ZX, Du XW, Wang WM, Fu ZY, Wang H. Preparation of B_4C–SiC composite ceramics through hot pressing assisted by mechanical alloying. Int J Refract Met Hard Mater. 2013;41:270–5.

[68] Zhang ZX, Du XW, Wang WM, Fu ZY, Wang H. Preparation and sintering of high active and ultrafine B_4C-SiC composite powders. J Inorg Mater. 2014;29(2):185–90.

[69] Zhang ZX, Du XW, Li ZL, Wang WM, Zhang JY, Fu ZY. Microstructures and mechanical properties of B_4C–SiC intergranular/intragranular nanocomposite ceramics fabricated from B_4C, Si, and graphite powders. J Eur Ceram Soc. 2014;34(10):2153–61.

[70] Suryanarayana C. Mechanical alloying and milling. Prog Mater Sci. 2001;46(1–2):1–184.

[71] Tang WM, Zheng ZX, Wu YC, Xu GQ, Jun LÜ, Liu JW, et al. Structural evolution of Si-50%C powder during mechanical alloying and heat treatment. Trans Nonferrous Met Soc China. 2008;18(4):865–71.

[72] Yang XY, Huang ZW, Wu YK, Ye HQ. HREM observations of the synthesized process of nano-sized SiC by ball milling of Si and C mixed powders. Mater Sci Eng A. 2001;300(1–2):278–83.

[73] Zhang ZX, Du XW, Wang JL, Wang WM, Wang YC, Fu ZY. Synthesis and structural evolution of B_4C–SiC nanocomposite powders by mechanochemical processing and subsequent heat treatment. Powder Technol. 2014;254:131–6.

[74] Kodera Y, Yamamoto T, Toyofuku N, Ohyanagi M, Munir ZA. Role of disorder-order transformation in consolidation of ceramics. J Mater Sci. 2006;41(3):727–32.

[75] Keçeli Z, Ögünç H, Boyraz T, Gökçe H, Addemir O, Öveçoğlu ML. Effects of B_4C addition on the micro-structural and thermal properties of hot pressed SiC ceramic matrix composites. J Achiev Mater Manuf Eng. 2009;37(2):428–33.

[76] Rocha RMD, Melo FCLD. Pressureless sintering of B_4C-SiC composites for armor applications. Ceram Eng Sci Proc. 2010;30(5):113–9.

[77] Rocha RMD, Melo FCLD. Sintering of B_4C-SiC composites with AlN-Y_2O_3 addition. Mater Sci Forum. 2012;727–728:850–5.

[78] Song SC, Bao CG, Wang B. Effect of the addition of carbon fibres on the microstructure and mechanical properties of reaction bonded B_4C/SiC composites. J Eur Ceram Soc. 2016;36(8):1905–13.

[79] Moshtaghioun BM, García DG, Rodríguez AD. High-temperature plastic deformation of spark plasma sintered boron carbide-based composites: The case study of B_4C–SiC with/without graphite (g). J Eur Ceram Soc. 2016;36(5):1127–34.

[80] Zhu Y, Wang FC, Wang YW, Cheng HW, Luo DJ, Zhao YZ. Mechanical properties and microstructure evolution of pressureless-sintered B_4C-SiC ceramic composite with CeO_2 additive. Ceram Int. 2019;45(12):15108–15.

[81] Zhu Y, Luo DJ, Li ZJ, Wang YW, Cheng HW, Wang FC, et al. Effect of sintering temperature on the mechanical properties and microstructures of pressureless-sintered B_4C/SiC ceramic composite with carbon additive. J Alloy Compd. 2020;820:153153.

[82] Moshtaghioun BM, Cumbrera FL, Ortiz AL, Rodríguez MC, García DG. Additive-free superhard B_4C with ultrafine-grained dense microstructures. J Eur Ceram Soc. 2014;34(3):841–8.

[83] Walker LS, Pinc WR, Corral EL. Powder processing effects on the rapid low-temperature densification of ZrB_2. J Am Ceram Soc. 2012;95(1):194–203.

[84] Levashov EA, Mukasyan AS, Rogachev AS, Shtansky DV. Self-propagating high-temperature synthesis of advanced materials and coatings. Int Mater Rev. 2017;62(4):203–39.

[85] Takacs L. Self-sustaining reactions induced by ball milling. Prog Mater Sci. 2002;47(4):355–414.

[86] Aruna ST, Mukasyan AS. Combustion synthesis and nanomaterials. Curr Opin Solid State Mater Sci. 2008;12(3–4):44–50.

[87] Jin HB, Li JT, Cao MS, Agathopoulos S. Influence of mechanical activation on combustion synthesis of fine silicon carbide (SiC) powder. Powder Technol. 2009;196(2):229–32.

[88] Morsi K. Combustion synthesis and the electric field: A review. Int J Self-Propag High-Temp Synth. 2017;26(3):199–209.

[89] Bowen CR, Derby B. Selfpropagating high temperature synthesis of ceramic materials. Br Ceram Trans. 1997;96(1):25–31.

[90] Roghani H, Tayebifard SA, Kazemzadeh A, Nikzad L. Effect of Mg/B_2O_3 molar ratio and furnace temperature on the phase evaluation and morphology of SiC-B_4C nanocomposite prepared by MASHS method. Mater Chem Phys. 2015;161:162–9.

[91] Roghani H, Tayebifard SA, Kazemzadeh A, Nikzad L. Effect of milling parameters on the phase transformations and morphology changes of B_4C-SiC nanocomposite powder *in situ* synthesized by MAVCS method. J Ceram Process Res. 2016;17(3):170–5.

[92] Roghani H, Tayebifard SA, Kazemzadeh A, Nikzad L. Phase and morphology studies of B_4C–SiC nanocomposite powder synthesized by MASHS method in B_2O_3, Mg, C and Si system. Adv Powder Technol. 2015;26(4):1116–22.

[93] Alkan M, Sonmez MS, Derin B, Yücel O. Effect of initial composition on boron carbide production by SHS process followed by acid leaching. Solid State Sci. 2012;14(11-12):1688–91.

[94] Nikzad L, Ebadzadeh T, Vaezi MR, Tayebifard A. Effect of milling on the combustion synthesis of ternary system B_2O_3, Mg and C. Micro Nano Lett. 2012;7(4):366–9.

[95] Demircan U, Derin B, Yücel O. Effect of HCl concentration on TiB_2 separation from a self-propagating high-temperature synthesis (SHS) product. Mater Res Bull. 2007;42(2):312–8.

[96] Roghani H, Tayebifard SA, Kasraee K, Asl MS. Volume combustion synthesis of B_4C–SiC nanocomposites in tubular and spark plasma furnaces. Ceram Int. 2020;46(18):28922–32.

[97] Novák P, Michalcová A, Školáková A, Průša F, Kříž J, Marek I, et al. Effect of heating rate on the formation of intermetallics during SHS process. Acta Phys Pol A. 2015;128(4):561–3.

[98] Mondal S, Banthia AK. Low-temperature synthetic route for boron carbide. J Eur Ceram Soc. 2005;25(2–3):287–91.

[99] Najafi A, Fard FG, Rezaie HR, Ehsani N. Effect of APC addition on precursors properties during synthesis of B_4C nano powder by a sol–gel process. J Alloy Compd. 2011;509(37):9164–70.

[100] Raman V, Bahl OP, Dhawan U. Synthesis of silicon carbide through the sol-gel process from different precursors. J Mater Sci. 1995;30(10):2686–93.

[101] Koc R, Glatzmaier G, Sibold J. β-SiC production by reacting silica gel with hydrocarbon gas. J Mater Sci. 2001;36(4):995–9.

[102] Najafi A, Fard FG, Rezaie HR, Ehsani N. Effect of APC addition on stability of nanosize precursors in sol-gel processing of SiC nanopowder. J Alloy Compd. 2010;505(2):692–7.

[103] Rahaman MN. Ceramic Processing. Boca Raton, USA: CRC Press; 2007.

[104] Najafi A, Fard FG, Rezaie HR, Saeb SP. Sol-Gel synthesis and characterization of SiC–B_4C nano powder. Ceram Int. 2021;47(5):6376–87.

[105] Tkachenko YG, Britun VF, Prilutskii ÉV, Yurchenko DZ, Bovkun GA. Structure and properties of B_4C-SiC composites. Powder Metall Met Ceram. 2005;44(3–4):196–201.

[106] Cihangir S, Ergun C, Yılmaz Ş, Şahin FÇ. Synthesis of B_4C/SiC composite from sugar based precursor. Defect Diffus Forum. 2009;283–286:268–72.